# Disproportionation of Toluene on ZSM5 Washcoated Monoliths

**B. Mitra, Jyoti Prasad Chakraborty, and Deepak Kunzru**
Dept. of Chemical Engineering, Indian Institute of Technology Kanpur, Kanpur 208016, India

*DOI 10.1002/aic.12531*
*Published online February 28, 2011 in Wiley Online Library (wileyonlinelibrary.com).*

*ZSM5 washcoated monoliths with zeolite loading ranging from 10 to 60 wt % were prepared, characterized, and examined for disproportionation of toluene. Toluene conversion increased with temperature and* $W/F_{Ao}$ *but decreased with washcoat thickness. The selectivity of the most desirable isomer (*p-*xylene) increased with a decrease in temperature,* $W/F_{Ao}$ *and washcoat thickness. The high selectivity to* p-*xylene indicates that the initially formed para isomer is easily removed from the zeolite pores in the thin washcoat to the bulk gas phase preventing further isomerization of the primary product. A reaction scheme has been proposed for this reaction and the kinetic parameters determined for the 10 wt % ZSM5 monolith. A one-dimensional reactor model was developed to predict the performance of the reactor for disproportionation of toluene. The model equations were coupled with a module to calculate the concentration profile in the washcoat by considering the effect of diffusion and reaction.* © 2011 American Institute of Chemical Engineers *AIChE J,* 57: 3480–3495, 2011
*Keywords: ZSM5, monoliths, toluene disproportionation,* para-*xylene selectivity, modeling*

## Introduction

Out of the several types of structured reactors that have been investigated as a means of process intensification, monoliths are the most widely used. Processes using monoliths have been commercialized for several gas–solid applications, such as treatment of automotive exhausts, stationary emission control, ozone abatement, catalytic incineration, etc.[1–3] Presently, there is growing interest in using monolith reactors (or monolith catalysts) for other gas–solid and gas-liquid-solid reactions in the chemical and process industry. These reactors have the advantage of high geometric surface area, low pressure drop, efficient mass transfer, enhanced thermal stability, high mechanical strength, high effectiveness factors, and ease of product separation.[2] A monolithic catalyst is made by either applying a layer of catalytically active material or an appropriate support (to be later loaded with the catalytically active component) on the walls of the monolith channels. Zeolites are a class of such catalytically active material, which may be coated on monoliths. The shape selective nature of zeolites and their acidity make these very attractive as solid acid catalysts.[4] Zeolites may be coated on the walls of the monolith reactor by washcoating the monoliths with a zeolite slurry or by hydrothermal synthesis of zeolite films on the walls. The advantage of the slurry washcoating method is its simplicity, the reactants need to diffuse only through a short distance to reach the active catalyst species and ready made catalysts can be deposited directly on the substrate. Shorter diffusional distances lead to higher catalyst efficiency for a fast reaction and a higher selectivity in case of multiple reactions.[5] Studies to optimize the washcoating technique for washcoating of zeolites on cordierite monoliths have been reported by Zamaro et al.[6] and Mitra and Kunzru.[7] Some of the gas-solid reactions that have been studied using zeolite washcoated

Correspondence concerning this article should be addressed to D. Kunzru at dkunzru@iitk.ac.in.
Current Address of B. Mitra: Department of Chemical Engineering, University. Institute of Engineering and Technology, CSJM University, Kanpur 208024, India.

monolithic reactors include SCR of $NO_x$, catalytic decomposition of $NO_x$, methanol to gasoline conversion, *n*-hexane cracking, ethylation of toluene, etc.[8–12]

The catalyst in a monolith reactor is located as a thin layer on the walls of the monolith structure and thus has a short diffusional distance. In a packed-bed reactor, the size of the catalyst particle needs to be reduced to reduce the diffusional length, which often leads to excessive pressure drop. In a monolith reactor, it is possible to simultaneously operate with a short diffusional length and a low pressure drop.[13] For the same reactor volume, the catalyst loading in a monolith reactor can be varied by changing the washcoat thickness. A change in the washcoat thickness also alters the linear velocity in the channels at constant feed rate as well as the diffusional distance and hence the product distribution in the case of a complex reaction network.[14,15] Very few experimental studies[14–16] have been reported on the effect of washcoat thickness on the activity and selectivity of monolith catalysts but none of these are on zeolite washcoated monoliths.

Research in the last few decades has shown that the shape selective properties of zeolites may be exploited for commercial processes in petroleum refining and petrochemical and chemical manufacturing.[17] Disproportionation of toluene to yield benzene and a mixture of xylenes is a commercially important reaction. This reaction is carried out over a variety of acid catalysts such as mordenite, zeolite Y, and ZSM5.[18–22] The reaction has been reported to proceed in two steps—the disproportionation reaction inside the zeolite pore to produce primary products of benzene and a mixture of xylenes (with a predominance of the smaller diameter and faster diffusing *p*-xylene) followed by isomerization reaction to yield the final xylene isomer mixture.[23] In most cases, the concentration of xylene isomers obtained is typically close to the thermodynamic equilibrium (24.4% *o*-xylene, 52.1% *m*-xylene, and 23.5% *p*-xylene at 700 K).[24] However, there is a need to maximize the production of the most valuable isomer, *p*-xylene, because it can be oxidized to terephthalic acid, which is used for making polyester films and fibers. In earlier studies, selectivity to *p*-xylene has been enhanced by modifying the ZSM5 catalysts with boron, magnesium, calcium, lanthanum, cerium or phosphorous, coke addition, and silica deposition.[23,25–27] These modifications result in high *p*-xylene selectivity but the activity of these modified ZSM5 catalysts is significantly lower as the active sites are also blocked during the modification process.

Depending on the reaction kinetics and catalyst properties, it may be possible to control the product distribution in monolith reactors by altering the thickness of the catalyst layer and hence the diffusional distance. For the disproportionation of toluene, the ZSM5 catalyst can be deposited as thin washcoats on the monolith walls. This would reduce the pore diffusional resistance of the reactants and products. A lower pore resistance would increase the rate of toluene reaction and may also help in preventing the isomerization of the initially formed *p*-xylene to other isomers and thereby enhance its selectivity. Furthermore, several mathematical models have been proposed to predict the behavior of monolith reactors. Chen et al.[28] published a comprehensive review on the mathematical modeling of monolith catalysts and reactors for the gas phase reactions. Depending on the objectives, one-dimensional, two-dimensional, or three-dimensional models have been used. Although modeling studies have been performed on several automobile and nonautomobile applications, to the best of our knowledge, there are no studies on the modeling of monolith reactors for the disproportionation of toluene.

The aim of this study is to investigate the feasibility of carrying out the toluene disproportionation reaction in a cordierite monolith washcoated with ZSM5 and to explore the possibility of increasing *p*-xylene selectivity by using a monolith reactor. The effect of temperature, contact time, and ZSM5 washcoat thickness on toluene conversion and product distribution was investigated. Based on the product distribution, a reaction scheme has been proposed and the kinetic constants for the reaction have been determined using a 10 wt % ZSM5 washcoated monolith. The intrinsic kinetics was then incorporated in a reactor model to predict the effect of washcoat thickness on the activity and product selectivities of toluene disproportionation conducted in a ZSM5 washcoated monolith reactor. Experimental data determined at different temperatures (573–773 K), $W/F_{Ao}$ (5–22 g h/mol), and washcoat thickness (18–144 $\mu$m) were used to validate the model.

## Experimental Procedure

### *Catalyst preparation*

Cordierite monoliths obtained from Corning (Shanghai, China) having 400 cells per square inch (cpsi) and average wall thickness of 0.19 mm were used as catalyst supports. Small sections of monoliths (diameter: 19.5 mm; length: $\sim$30 mm) were obtained by core-drilling from the larger blocks. These were washcoated with an aqueous slurry of ZSM5 (Si/Al = 34, $NH_4$ form, surface area = 348 $m^2/g$) obtained from Sud Chemie (Ahmedabad, India). Before washcoating, the monoliths were pretreated at 873 K for 2 h to remove any adsorbed impurities. The average particle size of the supplied ZSM5 powder was reduced to 2–3 $\mu$m by wet ball-milling in a Fritsch Planetary Mono Mill (Model: Pulverisette 6). The particle size of the powder was measured by the laser beam scattering technique using a Malvern Mastersizer 2000 Particle Size Analyzer. The slurry was prepared by mixing the ZSM5 powder with demineralized water in a ball-mill till a stable uniform slurry was formed. The monoliths were vertically immersed in a 30 wt % aqueous the slurry for 3 min, taken out, and the excess slurry removed from the channels by air blowing. The coated samples were dried at 383 K for 2 h and weighed. The coating process was repeated till the desired loading was reached. The zeolite loading was varied between 10 and 60 wt %. Zeolite washcoat loading was calculated as the weight of zeolite loaded per unit weight of the bare monolith. The samples were finally calcined at 823 K for 4 h at a heating rate of 2 K/min. A slow heating rate was used to minimize cracking of the washcoated layer. The adherence of the ZSM5 washcoat was determined by measuring the weight loss during ultrasonication. For this, the coated monoliths were immersed in acetone and treated in an ultrasound bath (33 kHz) for 1 h.

The morphology of the ZSM5 washcoated monoliths were examined by means of a scanning electron microscope (Model No JEOL 840A) operating at an accelerating voltage

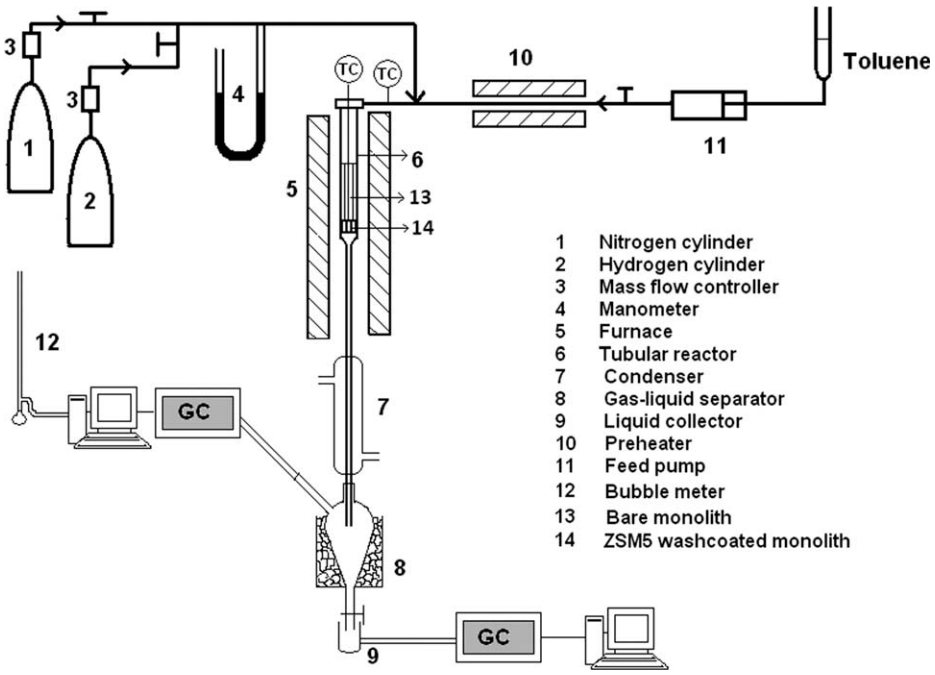


**Figure 1. Schematic diagram of the experimental setup.**

of 20 keV. The samples were coated with a thin layer of gold to improve the images and were glued to the sample holder by silver paint.

The surface area of the as-supplied ZSM5 powder and the washcoated monoliths was determined by nitrogen physisorption using the dynamic pulsing technique on a Micrometrics Pulse Chemisorb 2705 unit. The total flow rate of the gas (30% $N_2$ and 70% He) was maintained at 16 $cm^3$/min. To ensure complete removal of moisture, the samples were degassed in a flow of Ar (20 $cm^3$/min) at 723 K for 4 h before surface area determination.

The coke deposition on the catalyst after reaction was determined by thermogravimetric analysis in a TGA instrument (Model: Pyris Diamond, Perkin Elmer, USA). The used catalyst was heated from 303 to 973 K at 10 K/min in the presence of flowing oxygen and weight loss determined as a function of temperature.

### *Catalytic reaction studies*

Reaction studies on the monolith catalysts were carried out in a continuous downflow vertical reactor made of stainless steel (diameter = 19.7 mm, length = 320 mm) at atmospheric pressure. Another stainless steel tube (diameter = 3.2 mm, length = 330 mm) attached to the reactor served as the outlet to facilitate fast removal of the reactor effluents. The ZSM5 washcoated monolith was placed inside the reactor after the outer surface of the monolith piece was smoothened for a tight fit. A bare monolith piece (length = 125 mm) was placed before the active monolith piece to ensure fully developed flow of the reactants before these reach the catalyst piece. A thermocouple (Type K; diameter 0.5 mm) was introduced into the monolith channel at the centre of the catalyst piece for measuring the reaction temperature. A schematic diagram of the experimental setup is shown in Figure 1. Before each run, the monolith catalyst was treated in a stream of nitrogen (50 $cm^3$/min) at 823 K for 2 h. The temperature was then reduced to the reaction temperature. Toluene (Merck, purity 99.8%) was fed to a preheater through a pump (Model QG6, FMI Q Pump, USA) where it was vaporized at 473 K. The reaction was carried out in an atmosphere of hydrogen to reduce formation of coke. The vaporized feed was mixed with the hydrogen gas and then introduced into the reactor.

For the powder (120–85 mesh, diameter: 0.125–0.178 mm) and the pellet (diameter: 1.5 mm; length: 6 mm) catalysts, another stainless steel reactor (diameter: 7 mm; length: 550 mm) was used. The powder or pellet catalysts were placed on a bed of quartz wool and diluted with quartz particles to maintain adequate bed height.

The reaction was carried out in the temperature range of 573–773 K at different $W/F_{Ao}$ values. The $W/F_{Ao}$ was varied between 5 and 22 g h/mol. Toluene to hydrogen ratio of 1:2 was maintained for all the runs. Reaction runs were performed over monolith catalysts with different average washcoat thickness (18–144 $\mu$m). To ensure steady state, the product samples were collected 2 h after the toluene feed was introduced. The effluent from the reactor was condensed by passing the vapors through a condenser and collecting the liquid in a gas–liquid separator surrounded by ice. A bubble flow meter was used to measure the uncondensed gas flow rate and the amount of condensed liquid was measured at regular intervals. The gaseous and liquid products were analyzed by gas chromatography using a FID detector with nitrogen as the carrier gas. A Porapak QS (length 3 m) packed column and a 5% SP-1200/1.75% Bentone 34 on 100/120 Supelcoport column (length 3 m) was used to analyze the gaseous and liquid products, respectively. The carbon balance for all the reaction runs was within 100% $\pm$ 5%.

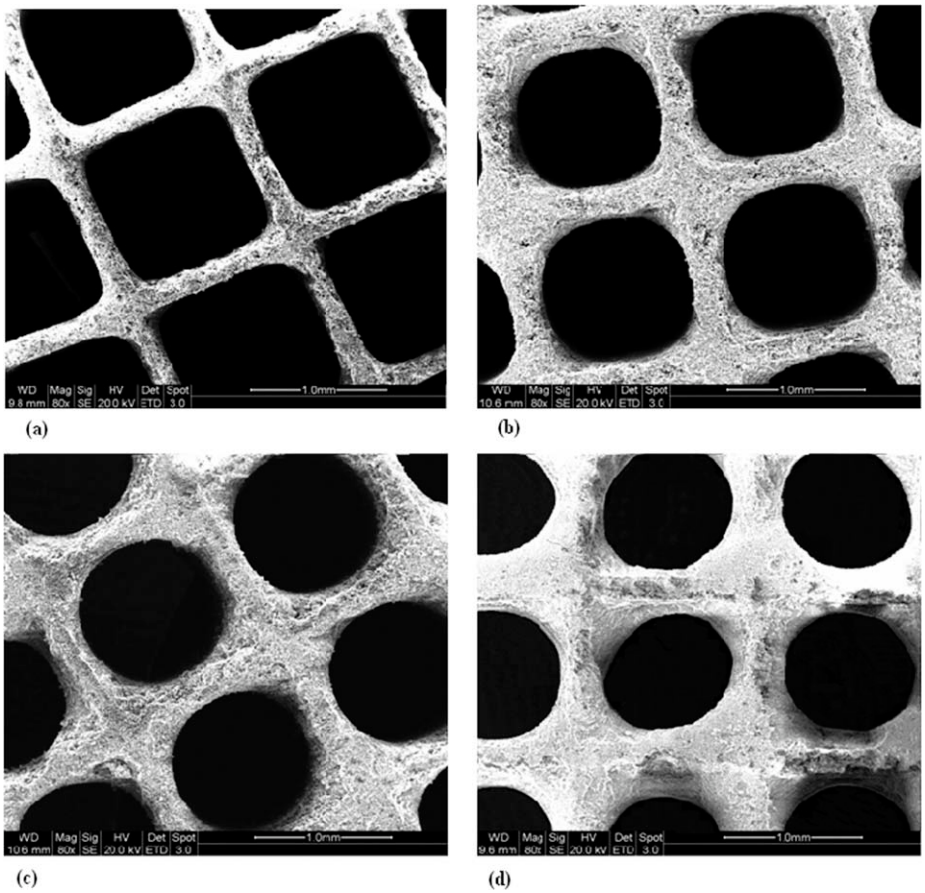


**Figure 2. SEM images of ZSM5 washcoated monoliths: (a) 10 wt %, (b) 28 wt %, (c) 41 wt %, and (d) 60 wt % loading.**

## Results and Discussion

### *Catalyst preparation and characterization*

The cordierite monoliths were washcoated with ZSM5 by the slurry method. Previous studies have shown that the characteristics of the zeolite washcoat layers depend on the properties of the slurry as well as that of the solid particles.[6,7] The use of a ZSM5 slurry of 30 wt % yielded washcoated monoliths with adequate homogeneity, reproducibility, and adherence.

The SEM images of ZSM5 washcoated monoliths of different loadings are shown in Figure 2. As can be seen from the figure, the washcoat thickness was maximum at the corners and minimum at the side walls of the monolith channel. Figure 3 shows the variation in the maximum and minimum thickness with an increase in ZSM5 loading as measured by SEM. Initially, the maximum thickness increased linearly with a higher slope than the minimum thickness, but at higher loadings the slopes were equal. During coating, initially, a larger portion of the zeolite accumulates at the corners as compared with the walls of the square channels. As the coating proceeds, the geometry of the channels becomes circular and accumulation of the zeolite at the corners decreases, resulting in the incremental increase in washcoat thickness at the corners and the walls becoming identical. The large variation in the magnitude of the maximum and minimum washcoat thickness using the slurry washcoating procedure was also observed by Zamaro et al.,[6] Hayes and Kolaczkowski,[29] and Zhang et al.[30] The expressions given by Vergunst et al.[14] were used to calculate the geometrical

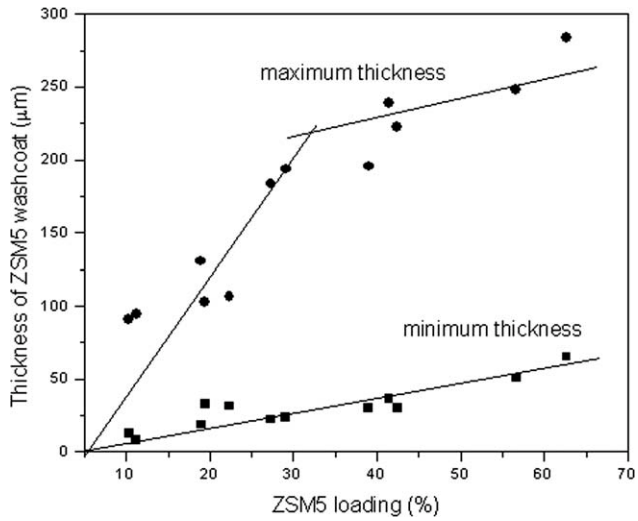


**Figure 3. Variation in maximum and minimum washcoat thickness with washcoat loading.**

**Table 1. Geometric Properties and Surface Area of the Different Washcoated Monoliths**

| ZSM5 Loading (wt %) | Minimum Washcoat Thickness ($\mu$m) | Maximum Washcoat Thickness ($\mu$m) | Corner Radius ($R$, $\mu$m) | Geometrical Surface Area ($a_m$, $m^{-1}$) | Void Fraction ($\varepsilon_m$) | Catalyst Volume Fraction ($x_c$) | Average Washcoat Thickness ($L_c$, $\mu$m) | Surface Area of ZSM5-Coated Monolith ($m^2$ $g^{-1}$) | $\frac{V^{\#}}{V_{cat}}$ (%) |
|---|---|---|---|---|---|---|---|---|---|
| 10 (±0.4) | 8.3 (±0.5) | 91.9 (±1.8) | 193.7 (±2.8) | 2578 (±6) | 0.67 (±0.00) | 0.05 (±0.00) | 18 (±0.9) | 31.8 (349.8)* | 24.2 |
| 19 (±0.6) | 16.9 (±0.6) | 116.9 (±2.4) | 224.6 (±6.4) | 2490 (±11) | 0.63 (±0.01) | 0.08 (±0.00) | 32 (±1.2) | 48.2 (301.9)* | 16.1 |
| 28 (±0.9) | 22.9 (±0.6) | 186.6 (±5.1) | 372.4 (±10.0) | 2273 (±16) | 0.56 (±0.01) | 0.15 (±0.01) | 66 (±3.2) | 62.8 (287.1)* | 13.1 |
| 41 (±1.7) | 31.8 (±2.9) | 215.3 (±8.4) | 411.0 (±10.5) | 2174 (±29) | 0.52 (±0.01) | 0.19 (±0.01) | 89 (±7.2) | 94.2 (324.0)* | 8.9 |
| 60 (±2.8) | 59.9 (±7.3) | 268.6 (±17.8) | 443.8 (±17.9) | 1971 (±64) | 0.43 (±0.03) | 0.28 (±0.03) | 144 (±19.0) | 118.3 (315.5)* | 3.0 |

*Values in parenthesis are surface area of ZSM5-coated monoliths calculated per gram. $\frac{V^{\#}}{V_{cat}}$ = Volume fraction of catalyst with thickness greater than the average washcoat thickness.

surface area ($a_m$), void fraction ($\varepsilon_m$), catalyst volume fraction ($x_c$), and average washcoat thickness ($L_c$). It should be mentioned here that the average washcoat thickness was calculated as the ratio of the volume fraction of the catalyst to the geometric surface area. All the above mentioned properties are a function of minimum and maximum thickness, channel diameter, corner radius, cell density, and channel wall thickness. With an increase in washcoat loading, $L_c$ and $x_c$ increased, whereas $a_m$ and $\varepsilon_m$ decreased. The values for different washcoat loadings, together with the variations, are shown in Table 1. As there was a significant difference in the diffusion length (washcoat thickness) along the sides and in the corners, the volume fraction of the catalyst that has a diffusion length longer than the average washcoat thickness has been calculated. This is denoted as $V^{\#}/V_{cat}$ in Table 1. This value ranged from 24% to 3% for the monolith loadings from 10 to 60 wt %, respectively.

Results of the adherence tests showed that the zeolite weight loss for monoliths with a loading less than 30 wt % was 1–2% and up to 5% for the higher loaded monoliths. Binders were not used during the washcoating process as our previous studies have shown that adhesion of the washcoat even without binders is sufficiently high.[7]

The surface area of the washcoated monoliths was estimated by the volume of nitrogen adsorbed and is given in Table 1. The surface area increased with an increase in zeolite loading in the washcoat. The surface area was essentially that of the ZSM5 washcoat layer as the surface area of the cordierite is ~0.7 $m^2$/g. A comparison of the surface area calculated per gram of ZSM5 (shown in parenthesis in Table 1) with the surface area of ZSM5 powder confirmed that particle size reduction, slurry preparation by wet ball-milling, and calcination steps result in only minor changes in the effective surface area of ZSM5. Similar results were obtained in our earlier study on different zeolites, including ZSM5.[7]

### *Catalytic reaction studies*

Blank runs, in the absence of any catalyst, were carried out and the contribution of homogeneous reactions was found to be negligible. Experiments with uncoated cordierite monoliths resulted in insignificant toluene conversions confirming that bare cordierite was not active for toluene disproportionation. The extent of deactivation of the ZSM5 washcoated monolith catalysts was tested by varying the time-on-stream up to 10 h at 773 K, and the decrease in toluene conversion with run time was found to be less than 1.5%. No coke deposition was observed at the end of the run as determined from TGA. To determine the effect of external mass transfer resistance, experimental runs were also carried out at a constant temperature of 773 K and $W/F_{Ao}$ = 10 g h/mol and total flow rates ranging between 35 and 250 $cm^3$/min. For these range of flow rates, the toluene conversion was constant, implying external diffusional resistance was negligible.

Toluene disproportionation reaction was carried out at atmospheric pressure on ZSM5 powder, ZSM5 pellets, and ZSM5 washcoated monoliths having different coating thickness. The conversion vs. $W/F_{Ao}$ data for the powder, 10 and 41 wt % ZSM5-coated monolith samples at different temperatures are shown in Figures 4a–c, respectively. Conversion vs. $W/F_{Ao}$ plots for washcoat loadings of 28 and 60 wt % at 723 K are given later (Figure 8). As expected, for both powder and monolith catalysts, conversion of toluene increased with an increase in temperature and $W/F_{Ao}$. The major products obtained were benzene, *p*-xylene, *m*-xylene, *o*-xylene, and gaseous hydrocarbons (methane, ethane, ethylene, and propylene). Low concentrations of ethylbenzene and $C_{9+}$ aromatics were also observed in the products but were neglected in the analysis owing to their insignificant amounts. When comparing Figures 4b, c, it can be noticed that, at identical conditions, the conversion was lower on 41% washcoated monoliths. The product distribution for 10 and 41 wt % washcoated monoliths at different temperatures is given in Table 2. Similar reaction products were obtained on powder and pelletized catalysts by previous workers.[26,31]

From stoichiometry, when toluene disproportionates, equimolar concentrations of benzene and xylenes should be present in the products, but the presence of gaseous hydrocarbons in the effluent gases reveals that secondary dealkylation reaction also takes place along with disproportionation. The benzene to xylene ratio in these experiments was very close to 1 and increased with an increase in temperature and space time, indicating that the presence of xylenes was required for larger amounts of gaseous hydrocarbons to be formed, as was also observed by Uguina et al.[31] and Bhaskar and Do.[32]

The influence of washcoat thickness on the conversion of toluene at different temperatures and at a constant $W/F_{Ao}$ (10 g h/mol) is shown in Figure 5. For comparison, the conversion data for the powder and pellet samples are also shown in the same figure. To obtain a constant $W/F_{Ao}$, the toluene flow rate was changed according to the amount of catalyst in the 30-mm long coated monolith. At identical conditions, similar conversions were obtained with the ZSM5 powder and monoliths loaded with 10 and 19 wt %

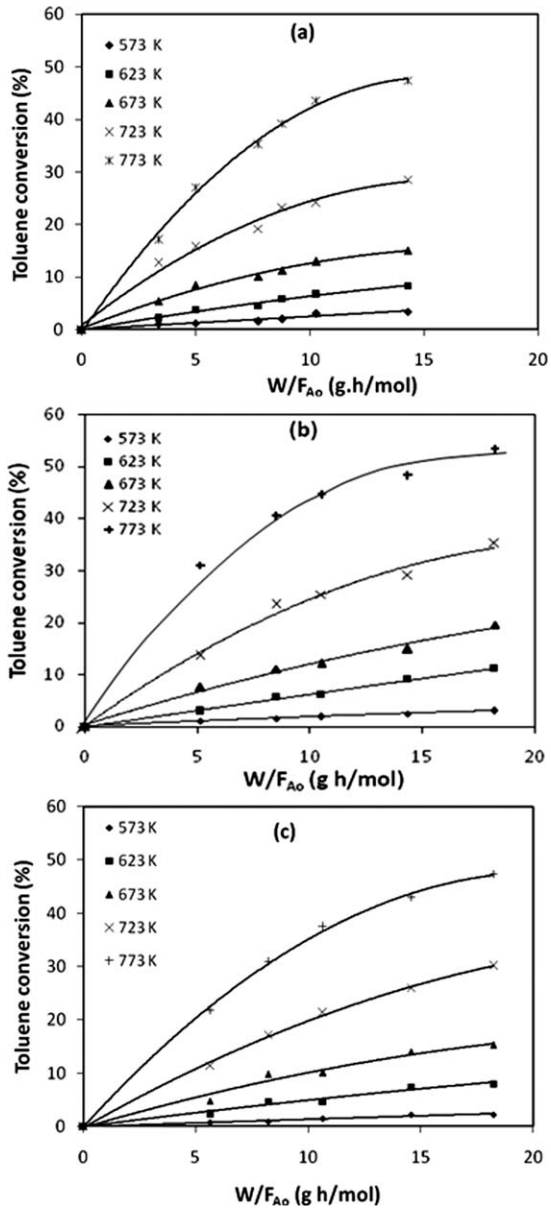


**Figure 4. Conversion vs. $W/F_{Ao}$ for ZSM5-coated monolith samples at different temperatures: (a) Powder catalyst, (b) 10 wt % ZSM5-coated monolith, and (c) 41 wt % ZSM5-coated monolith.**

ZSM5. However, at higher loadings, conversion decreased with an increase in washcoat thickness. The data suggests that beyond a loading of 19%, the conversion is affected by diffusional resistances. As for the pellet samples, the larger characteristic diffusion length and the presence of binder further reduced the conversion of toluene.

Figures 6a, b show the variation in *p*-xylene to *o*-xylene ratio and *p*-xylene to *m*-xylene ratio with conversion at 573 K for monoliths at different washcoat loadings of ZSM5, powdered, and pellet catalyst. The thermodynamic equilibrium concentration of xylene isomers at 573 K is 22.5% *o*-xylene, 53.4% *m*-xylene, and 24.1% *p*-xylene. Therefore, at equilibrium, the ratio of *p*-xylene to *o*-xylene should be ~1.1 and that of *p*-xylene to *m*-xylene should be ~0.45. These are shown as dotted lines in Figure 6. For all the monolith samples, the para-selectivity was higher than the equilibrium value and decreased with an increase in washcoat thickness. The *p*-xylene to *o*-xylene and *p*-xylene to *m*-xylene ratios of the 19 wt % loaded monoliths were similar to the 10 wt % loaded monoliths but are not shown here for the sake of clarity. It should be noted that the *p*-xylene to *o*-xylene ratio and the *p*-xylene to *m*-xylene ratio for the powdered catalyst were lower than for the 10 wt % loaded monolith. This could be due to some diffusional resistance in the transport of the products from the interior of the powdered catalyst or the different catalyst bed configuration. As can be seen from the figure, the experimental ratios were substantially different from the equilibrium values. The high values for para to ortho and para to meta ratios indicate that *p*-xylene is probably the first isomer formed. The initial nonequilibrium mixture of the three isomers further reacts to form the equilibrium mixture of the three xylene isomers. Nayak and Riekert[33] have previously reported that thermodynamically as well as kinetically, *p*-xylene is the most favored compound in the xylene mixture and it later isomerizes to yield the equilibrium mixtures of the three isomers. It was also observed that the ratio of para to ortho and para to meta decreased with an increase in temperature. The isomerization activity is enhanced with temperature and the difference in the diffusion rates of both *p*-xylene and *o*-xylene, and *p*-xylene and *m*-xylene decrease leading to the change in the ratios.[34]

In the washcoated monoliths, the catalyst is present as thin layers on the cordierite walls resulting in more zeolite channel openings being exposed for reactant entrance and product exit.[12] *p*-Xylene has the smallest molecular diameter amongst the three isomers and a configurational diffusivity which is 1000 times more than that of the meta and ortho isomers.[23] Thus, it can diffuse out of the ZSM5 pores as soon as it is formed into the bulk phase without getting a chance to isomerize further. As the washcoating thickness increases, the diffusional path length becomes longer. With increasing transport limitations, the selectivity to *p*-xylene decreases as it has a chance of being readsorbed and isomerized further. Kunnieda et al.[35] reported that in the toluene disproportionation reaction, selectivity to *p*-xylene formation was not governed by the first disproportionation step but the subsequent step of diffusion or isomerization of product xylene was controlling.

### *Reaction scheme*

The toluene disproportionation reaction essentially produces benzene, xylenes, and gaseous hydrocarbon as the products. For all the reaction runs, it was observed that among the three xylene isomers, *p*-xylene was formed predominantly at low conversions. Thus, the first reaction in the reaction scheme was assumed to be the conversion of toluene to benzene and *p*-xylene as shown in Eq. 1 below. This *p*-xylene may then form meta and ortho isomers either by a series or a triangular network. There is a general agreement that the isomerization reaction between xylene isomers occurs via the 1,2 shift of the methyl group.[23,36,37] Transformation of *p*-xylene into *o*-xylene (or vice versa) directly is not feasible and can be only through the *m*-xylene intermediate. Therefore, the next two reactions were taken to be the formation of *m*-xylene from *p*-xylene and formation of *o*-xylene from *m*-xylene as shown in Eqs. 2 and 3 below. The

**Table 2. Product Distribution for 10 and 41 wt % Washcoated Monoliths at Different Temperatures ($W/F_{Ao}$ = 10 g h/mol)**

| Washcoat Loading | 10 wt % | 41 wt % | 10 wt % | 41 wt % | 10 wt % | 41 wt % | 10 wt % | 41 wt % | 10 wt % | 41 wt % |
|---|---|---|---|---|---|---|---|---|---|---|
| Temperature (K) | 573 | | 623 | | 673 | | 723 | | 773 | |
| Conversion (%) | 1.91 | 1.42 | 6.18 | 4.63 | 12.09 | 10.05 | 25.41 | 21.33 | 44.66 | 37.47 |
| Products | mol % | | mol % | | mol % | | mol % | | mol % | |
| Methane | 0.01 | 0.08 | 0.01 | 0.15 | 0.03 | 0.22 | 0.07 | 0.24 | 0.21 | 0.28 |
| Ethane | 0.01 | 0 | 0.05 | 0.09 | 0.13 | 0.14 | 0.31 | 0.16 | 0.83 | 0.17 |
| Ethylene | 0.02 | 0.06 | 0.04 | 0.15 | 0.06 | 0.41 | 0.06 | 0.52 | 0.10 | 0.94 |
| Propylene | 0.40 | 0.32 | 0.74 | 0.35 | 0.71 | 0.48 | 0.71 | 0.59 | 0.72 | 0.60 |
| Benzene | 48.59 | 48.64 | 48.43 | 48.98 | 48.68 | 49.13 | 48.78 | 49.40 | 50.22 | 49.63 |
| Ethylbenzene | Trace | 0.03 | 0.01 | 0.04 | 0.01 | 0.05 | 0.01 | 0.06 | 0.02 | 0.09 |
| *p*-Xylene | 25.11 | 22.21 | 18.84 | 16.67 | 17.46 | 15.17 | 14.35 | 13.85 | 13.13 | 12.95 |
| *m*-Xylene | 20.78 | 23.08 | 24.74 | 25.22 | 24.80 | 25.25 | 26.04 | 25.02 | 24.71 | 24.38 |
| *o*-Xylene | 5.06 | 5.54 | 7.11 | 8.28 | 8.06 | 9.07 | 9.58 | 9.92 | 9.97 | 10.85 |
| $C_{9+}$ compounds | 0.02 | 0.04 | 0.03 | 0.07 | 0.06 | 0.08 | 0.08 | 0.09 | 0.10 | 0.11 |

gaseous hydrocarbons in the product are formed by dealkylation reaction of either toluene or xylene. Previous work by Uguina et al.[31] on powder ZSM5 catalyst using *p*-xylene as feed showed that *p*-xylene, apart from isomerizing into *m*- and *o*-xylene, forms a large portion of toluene and gaseous hydrocarbon and a very small amount of benzene. This essentially reveals that *p*-xylene dealkylates to a great extent. In the toluene disproportionation reaction, benzene is formed as a primary product and not due to dealkylation of toluene. Hence, it can be concluded that the gaseous hydrocarbons formed were mainly due to dealkylation of *p*-xylene. Based on this, the reaction scheme proposed for the toluene disproportionation reaction in washcoated monoliths is

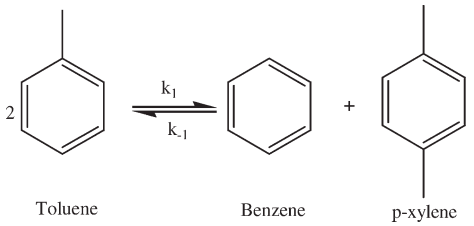


(1)

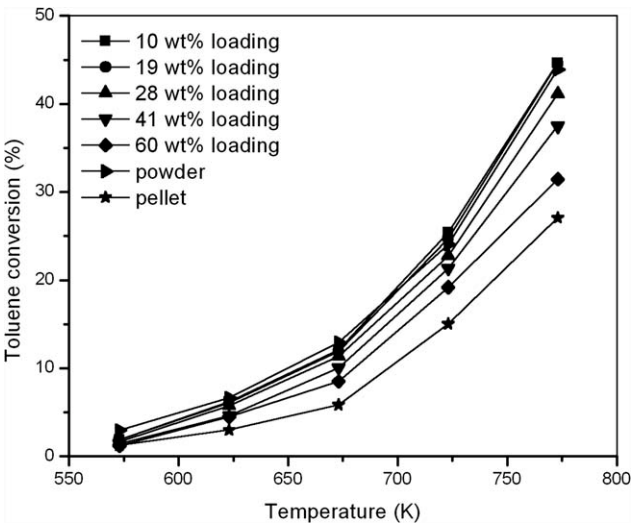


**Figure 5. Influence of washcoat thickness on the conversion of toluene at different temperatures ($W/F_{Ao}$ =10 g h/mol).**

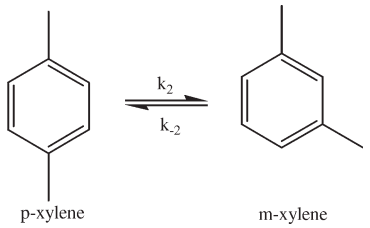


(2)

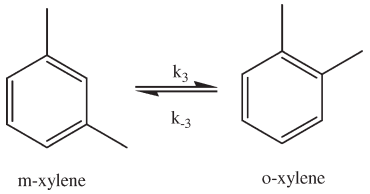


(3)

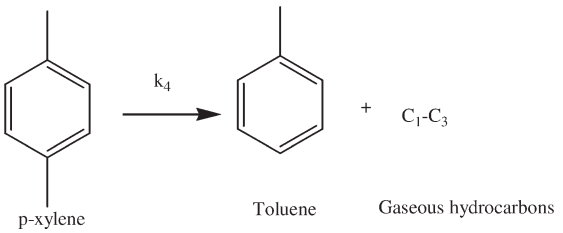


(4)

The first 3 reactions are reversible while the dealkylation step is an irreversible one. The rate expressions were written assuming that for all the reactions, the order corresponded to the stoichiometric coefficients. Uguina et al.[31] also assumed similar equations for the kinetic modeling of the toluene disproportionation reaction. The rate expressions of the four reactions given above are as follows:

$$r_1 = k_1\left(p_T^2 - \frac{p_B p_{PX}}{K_1}\right) \quad (5)$$

$$r_2 = k_2\left(p_{PX} - \frac{p_{MX}}{K_2}\right) \quad (6)$$

$$r_3 = k_3\left(p_{MX} - \frac{p_{OX}}{K_3}\right) \quad (7)$$

$$r_4 = k_4 p_{PX} \quad (8)$$

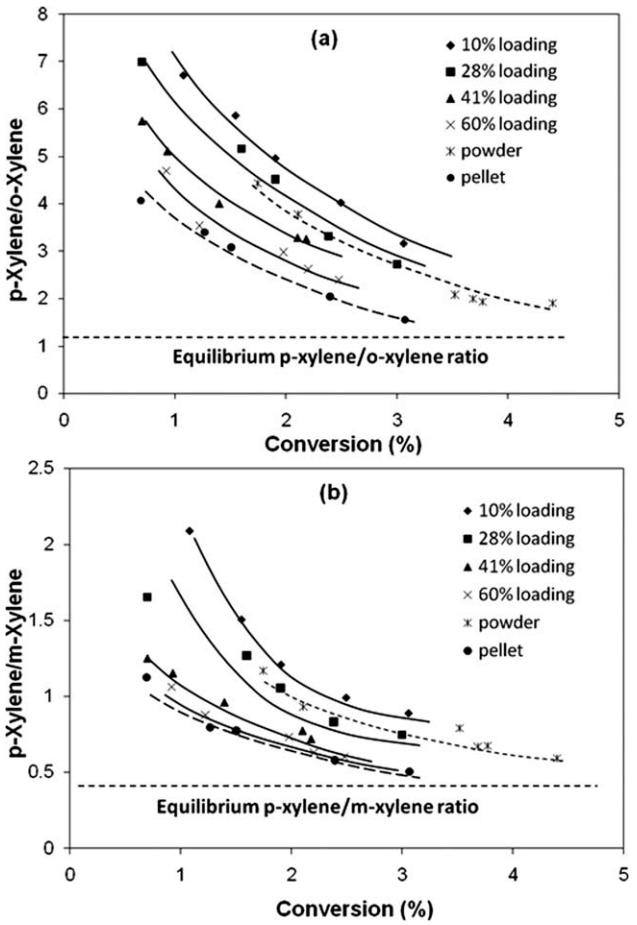


**Figure 6. Variation of molar ratio of *p*-xylene to *o*-xylene and *m*-xylene with $W/F_{Ao}$ for ZSM5 washcoated monoliths at different washcoat loadings (Temperature: 573 K): (a) *p*-Xylene/*o*-xylene and (b) *p*-xylene/*m*-xylene.**

Based on the rate expressions given above, the net rates of formation of the different species are as follows:

$$R_T = -2r_1 + r_4 \quad (9)$$

$$R_B = r_1 \quad (10)$$

$$R_{PX} = r_1 - r_2 - r_4 \quad (11)$$

$$R_{MX} = r_2 - r_3 \quad (12)$$

$$R_{OX} = r_3 \quad (13)$$

$$R_{GH} = r_4 \quad (14)$$

### *Intrinsic kinetics*

It was observed from Figure 5 that the conversions for the 10 wt % (average washcoat thickness = 18 $\mu$m) and 19 wt % (average washcoat thickness = 32 $\mu$m) loaded monoliths were equal and with further increase in washcoat thickness, the conversion declined. This data shows that in these low loading catalysts, diffusional resistances do not affect the measured rate of reaction and the kinetic constants determined for the 10 wt % loaded samples will be the intrinsic values. The para selectivity for the powder catalyst (average diameter = 152 $\mu$m) was lower than that for the 10 and 19 wt % loaded monoliths, although the conversions were similar (refer Figures 5 and 6). Hence, rate from the powder catalyst experiments were not used for determination of intrinsic kinetics.

The experimental net rates of formation of the different species ($R_i$) were obtained from the slopes of the plot of the mole fraction of the different product species vs. $W/F_o$. The equilibrium constants, $K_i'$s, for the three reaction steps (Eqs. 5–7) at different temperatures were estimated from the Gibbs free energy change of the respective reaction which was calculated from the standard Gibbs free energy of formation of the products and reactants.[38] The rates of the individual reactions ($r_1$–$r_4$) were calculated from the species reaction rates by simultaneously solving Eqs. 9–14. The rate constants ($k_1$–$k_4$) for the individual reactions at five different temperatures were estimated by nonlinear regression of the experimental rates and partial pressures of the reactant and product species by Levenberg-Marquardt method using Polymath 5.1. The values of the pre-exponential factor and the activation energy of the different reactions, together with their 95% confidence limits, are tabulated in Table 3. A comparison between the experimental rates and those calculated using the estimated kinetic parameters for the four reaction steps is shown in Figure 7. A reasonably good agreement was observed between the predicted and the experimental rates with $R^2$ values ranging from 0.898 to 0.985.

The activation energy calculated for the first disproportionation step is within the range of 65–99 kJ/mol reported by other investigators over ZSM5.[20,26,31,39] The activation energy for the *p*-xylene isomerization step was higher than the value of 21.43 kJ/mol reported by Li et al.[40] For washcoated monoliths, higher activation energy for the *p*-xylene isomerization step implies that the formation of *m*-xylene from *p*-xylene is relatively difficult, which is supported by the high para selectivity. The activation energy for the *m*-

**Table 3. Kinetic Parameters for the Toluene Disproportionation Reaction**

| | Activation Energy (J/mol) | | Pre-Exponential Factor | |
|---|---|---|---|---|
| Reaction | Value | 95% Confidence Limit | Value | 95% Confidence Limit |
| $2T \underset{k_{-1}}{\overset{k_1}{\rightleftarrows}} B + PX$ | 85,570 | 538.8 | $6.94 \times 10^{-6}$ mol/kg s Pa$^2$ | $2.11 \times 10^{-7}$ |
| $PX \underset{k_{-2}}{\overset{k_2}{\rightleftarrows}} MX$ | 33,060 | 176.9 | $1.03 \times 10^{-3}$ mol/kg s Pa | $9.17 \times 10^{-5}$ |
| $MX \underset{k_{-3}}{\overset{k_3}{\rightleftarrows}} OX$ | 41,460 | 878.1 | $1.19 \times 10^{-3}$ mol/kg s Pa | $5.51 \times 10^{-5}$ |
| $PX \overset{k_4}{\rightarrow} T + GH$ | 42,146 | 1736.5 | $3.08 \times 10^{-4}$ mol/kg s Pa | $5.87 \times 10^{-5}$ |

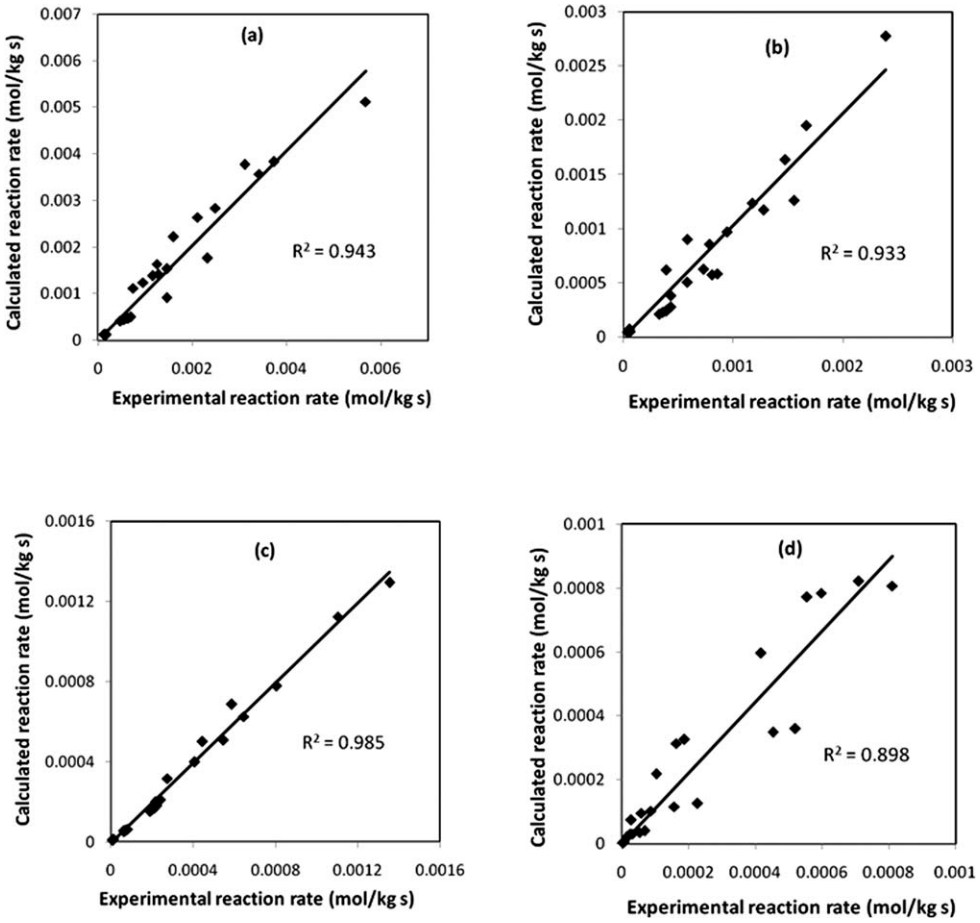


**Figure 7. Comparison between the calculated and experimental reaction rates for different reaction steps: (a) Toluene disproportionation, (b) *p*-xylene isomerization, (c) *m*-xylene isomerization, and (d) dealkylation of *p*-xylene.**

xylene isomeization step reported by Li et al.[40] and Al-Khattaf[34] were 46.29 and 43.33 kJ/mol, respectively, and this matches well with the data in this work. Li et al.[40] also reported an activation energy of 47.45 kJ/mol for the *p*-xylene dealkylation step. In this study, the activation energy of dealkylation (42.2 kJ/mol) is greater than for *p*-xylene isomerization (33.1 kJ/mol). This is expected as the energy required to remove a methyl group should be higher than a 1,2 intramolecular methyl transfer.[40]

### *Reactor model*

A large number of monolith reactor models with varying degrees of complexity have been developed by different researchers.[28] One-dimensional reactor models have been successfully used to understand the behavior of monolith reactors for reactions such as selective catalytic reduction of $NO_x$,[41,42] methanation of carbon monoxide,[43] methanol to gasoline,[11] automobile catalytic converters,[44,45] etc. The concentration and temperature profiles along the axial direction were usually considered in a one-dimensional model. In most of these cases, the pore diffusional resistance within the catalyst layer was assumed to be negligible.[45] Later studies have shown that neglecting internal mass transfer limitations can lead to erroneous conclusions regarding the performance of monolith reactors.[46–48]

In this study, a one-dimensional model was developed for the monolith reactor. The effect of washcoat thickness was studied by considering the diffusion and reaction inside the washcoat layer.

The different assumptions used in the mathematical model are as follows:

1. The reactor operates under isothermal and steady-state conditions. The heat of reaction for the toluene disproportionation reaction is very small (−2.3 kJ/mol at 773 K).

2. The flow is fully developed in all but a small section at the channel inlet of the reactor. According to Irandoust and Andersson,[3] the length required to obtain a fully developed concentration profile can be estimated from, $z/d = 0.05\ Sc\ Re$. In case of the experiments in this study, this length is ~0.05 mm.

3. The axial velocity of the gases is equal in all the channels of the monolith.

4. A plug flow reactor model is assumed, i.e., there are no concentration or velocity gradients in the radial direction in the open area of the monolith channels. A criterion based on superficial gas velocity, channel diameter, reactor length, and geometry has been published by Berger and Kapteijn[49] for estimating the influence of radial mass transport on the conversion on washcoated monoliths. This criterion showed that, for the experimental runs in this study, radial concentration gradients were absent.

5. The gas phase reactions are negligible and reaction occurs only in the zeolite washcoat. The catalytic activity is uniformly distributed throughout the coating layer and the deactivation of the catalyst is insignificant.

6. There is no transfer of mass between adjacent monolith channels.

The differential mass balance equations for each species, $i$, participating in $j$ reactions, in the axial direction $z$ of the monolith reactor is given by

$$\frac{dF_i}{dz} = A\rho_B R_i \eta_i; \quad i = 1-6 \tag{15}$$

where 1: toluene, 2: benzene, 3: *p*-xylene, 4: *m*-xylene, 5: *o*-xylene, 6: gaseous hydrocarbons

$$R_i = \sum_j \alpha_{ij} r_j; \quad j = 1-4 \tag{16}$$

$$\text{Boundary condition: } F_i = F_{i0} \text{ at } z = 0 \tag{17}$$

In the model, internal diffusion inside the monolith washcoat was considered along with catalytic reactions. The intrinsic rate expressions determined earlier were used for calculating the effectiveness factors for the monolith reactor. The catalyst washcoat was assumed to be a slab with the average washcoat thickness ($L_c$) as the characteristic length. This assumption was justified by the observations of Roy et al.[50] They determined the relationship between effectiveness factor and Thiele modulus for monoliths of different shapes and found that when characteristic length is defined as the ratio of catalyst volume fraction to the external surface area, the effectiveness factor vs. Thiele modulus plot for monoliths with square and round geometries and that for the slab and sphere pellet configuration collapse to the same curve. For catalyst effectiveness, the slab correlation seems to be universally applicable for monoliths of all shapes.

The mass balance of any species, $i$, across a slice of washcoat of thickness, $dx$, at an axial position $z$ results in a second-order differential equation in the $x$ direction, where $x$ is the dimensionless coordinate normal to the washcoat.

$$D_{e,i}\frac{d^2C_i}{dx^2} = -\rho_c {L_c}^2 R_i; \quad i = 1-6 \tag{18}$$

where $R_i$ is given by Eqs. 9–14

$$\text{and} \quad C_i = \frac{F_i}{\sum F_i + F_{H_2}} \times \frac{P}{RT} \tag{19}$$

For use in Eq. 18, the intrinsic rates of Eqs. 5–8 were expressed in terms of concentration of the species.

The boundary conditions for Eq. 18 are

$$C_i = C_{i,b} \quad \text{at} \quad x = 0 \tag{20}$$

$$\text{and} \quad \frac{dC_i}{dx} = 0 \quad \text{at} \quad x = 1 \tag{21}$$

Also, the effectiveness factor for each reaction can be evaluated as

$$\eta_j = \frac{\int_{x=0}^{x=1} r_j(C_i, T)dx}{r_j(C_{i,b}, T)} \tag{22}$$

The effectiveness factor for each species can be estimated from

$$\eta_i = \frac{\int_{x=0}^{x=1} R_i(C_i, T)dx}{R_i(C_{i,b}, T)} \tag{23}$$

where $R_i$ is given by Eq. 16.

Thus, Eq. 15 can also be written as

$$\frac{dF_i}{dz} = A\rho_B \int_{x=0}^{x=1} R_i(C_i, T)dx \tag{24}$$

The set of ordinary differential equations for the reactor (Eq. 24) was solved using the Runge-Kutta algorithm to obtain the molar flow rates of the six species, benzene, toluene, *p*-xylene, *m*-xylene, *o*-xylene, and gaseous hydrocarbons, at the outlet of the reactor. These were coupled with the module to solve the mass-balance equations inside the washcoat at each incremental $\Delta z$. The catalyst mass-balance equations (Eq. 18) were converted to a system of coupled nonlinear algebraic equations using the orthogonal collocation technique. The algebraic equations are given below.

$$D_{e,i}\sum_{k=1}^{N+2} B_{ik}C_{i,k} + \rho_c L^2 R_{i,k} = 0 \tag{25}$$

$$\text{where} \quad R_{i,k} = \sum_j \alpha_{ij} r_{j,k} \tag{26}$$

$$\text{with the boundary conditions: } C_{i,N+2} = C_{i,b} \text{ at } x = 0 \tag{27}$$

$$\text{and} \quad \sum_{k=1}^{N+2} A_{ik}C_{i,k} = 0 \text{ at } x = 1 \tag{28}$$

The concentration profile of all the species in the washcoat was estimated at five collocation points in the washcoat. Use of higher number of collocation points did not appreciably affect the concentration profile. The values of the elements of the matrices $A_{ik}$ and $B_{ik}$ in Eqs. 25 and 28 were determined using the procedure given in Gupta.[51] The values of the concentrations of the species determined at each collocation point were used to calculate the rate of each reaction at every collocation point (Eqs. 5–8). The reaction rates determined at each collocation point were subsequently used to obtain the volume averaged rates of the four reactions in the washcoat using the quadrature weightage values, as

$$\sum_{k=1}^{N+2} \omega_{ik} r_{j,k} = r_j \tag{29}$$

where $\omega_{ik}$ is the quadrature weightage.[51]

The rates of formation of the different species were calculated using volume averaged rates of the individual reactions using Eqs. 9–14. These rates for the species were then used for mass-balance equation for the reactor (Eq. 24). The effective diffusivities of the different species ($D_{e,i}$) were used as adjustable parameters and the optimal values were

determined by minimizing the residual sum of squares between the calculated and experimental exit molar flow rates of toluene, benzene, *p*-xylene, *m*-xylene, *o*-xylene, and gaseous hydrocarbons over all the runs.

The objective function was defined as

$$\mathrm{OBJ} = \sum_{k=1}^{15} \sum_{i=1}^{6} \left( \frac{F_i^{\mathrm{exp\,tal}} - F_i^{\mathrm{calculated}}}{F_i^{\mathrm{calculated}}} \right)^2 \quad (30)$$

Levenberg-Marquardt algorithm was used to minimize the objective function. All the calculations were performed using codes written in Matlab. The code was initially tested with a first-order reaction in the monolith reactor and the results were found to match with the analytical solution.

The conversion and product selectivity in monolith reactors may be influenced by both external and internal mass transfer limitations. As was stated earlier, the external mass transfer resistance was found to be negligible in this study. The washcoated monoliths were prepared by coating with a slurry of ZSM5 particles having an average diameter of 2–3 $\mu$m. These particles were made up of smaller ZSM5 crystals. In such a washcoat, most of the catalytic sites reside inside the zeolite crystals, and the transfer of the gaseous reactant from the bulk gas to the interior of the zeolite crystals will consist of three steps: diffusion through the pores of the washcoat to the surface of the particles, diffusion through the pores between the zeolite crystals (intercrystalline diffusion), and the diffusion through the micropores of the zeolite crystal (intracrystalline diffusion). The transfer of the products from the interior of the zeolite crystals to the bulk gas phase will follow a reverse path. The influence of intracrystalline diffusion in the zeolite crystals on the observed kinetics was estimated using the Weisz Prater criterion with the zeolite crystal size as the characteristic length. This criterion states that, to ensure $\eta > 0.95$ in an isothermal catalyst particle with first-order reaction,

$$\frac{R_{\mathrm{obs}} r_{\mathrm{p}}^2}{C_{\mathrm{s}} D_{\mathrm{e}}} < 1 \quad (31)$$

Weisz later showed that for a second-order reaction the numerical value of the right-hand side in the above equation is 0.3.[52]

The highest toluene disproportionation rate obtained in this study was at a temperature of 773 K and $W/F_{\mathrm{Ao}}$ of 5 g h/mol. At these reaction conditions, the toluene disproportion rate ($R_{\mathrm{obs}}$) in the monolith with a washcoat thickness of 18 $\mu$m was $1.658 \times 10^{-2}$ kmol/m$^3$ s. The surface concentration of toluene was $5.25 \times 10^{-3}$ kmol/m$^3$ and the average crystal size of the ZSM5 as determined from XRD was 37.34 nm. The effective diffusivity to be used in the Weisz-Prater criterion is difficult to determine as it may be influenced by surface diffusion, adsorption, and configurational diffusion. The contribution from surface diffusion becomes significant when the temperatures are low and there is considerable physical adsorption.[53] The temperatures used in this study (573–773 K) were much higher than the boiling point of toluene (383 K) and the molecules are likely to be chemisorbed. Therefore, surface diffusion which is significant at low temperatures may not be important here and its influence on effective diffusivity was neglected. However, adsorption affects the effective diffusivity in the zeolite crystals. As discussed by Xiao and Wei[54] and Masuda,[55] the effective diffusivity in the zeolite channels, $D_{\mathrm{e}}$, is related to the configurational (intracrystalline) diffusivity, $D_{\mathrm{con}}$, and the partition factor, $H$, as

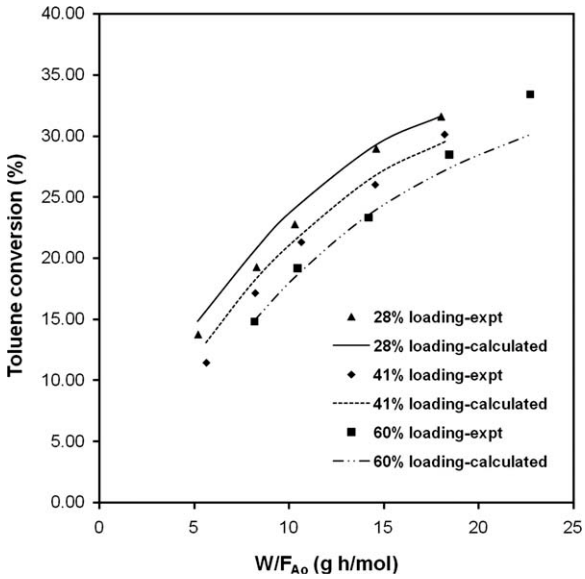


**Figure 8. Experimental and calculated toluene conversions at different $W/F_{\mathrm{Ao}}$ for monoliths with 28, 41, and 60 wt % loading (Temperature: 723 K).**

$$D_{\mathrm{e}} = H \times D_{\mathrm{con}} \quad (32)$$

where $H$ is the ratio of the concentration of the adsorbate molecule in zeolite crystals to that in the gas phase. $H$ decreases with temperature, whereas $D_{\mathrm{con}}$ increases with temperature. The activation energy of effective diffusivity is given by $(E + \Delta H)$ where $E$ is the activation energy of configurational diffusivity and $\Delta H$ is the heat of adsorption. The variation of $D_{\mathrm{e}}$ with temperature depends on the relative magnitudes of the activation energy of configurational diffusion and the heat of adsorption. From the data of Masuda and Hashomoto,[56] the value of $H$ for toluene on ZSM5 at 573 K was estimated as 852.7, and the adsorption enthalpy of toluene on ZSM5 has been reported to be $-54$ kJ/mol.[57] Using the data of Masuda et al.,[57] the configurational diffusivity of toluene on MFI type zeolite ($SiO_2/Al_2O_3$ ratio = 40) at 573 K was approximated as $1.8 \times 10^{-14}$ m$^2$/s, and the activation energy for configurational diffusivity for toluene in ZSM5 was estimated to be 46 kJ/mol. Thus, $D_{\mathrm{e}}$ for use in Eq. 31 for the zeolite channels could be expressed as,

$$D_{\mathrm{e}}\left(\mathrm{m}^2/\mathrm{s}\right) = 1.53 \times 10^{-11} \exp\left[962.23\left(\frac{1}{T} - \frac{1}{573}\right)\right] \quad (33)$$

According to Eq. 33, $D_{\mathrm{e}}$ decreases slightly with temperature and the value at 773 K was $9.91 \times 10^{-12}$ m$^2$/s. Similar dependency of effective diffusivity with temperature has been reported for benzene in zeolite Y and mordenite, ethane in $\beta$ zeolite, and hexane and decane in zeolite Y.[55,58] The effective

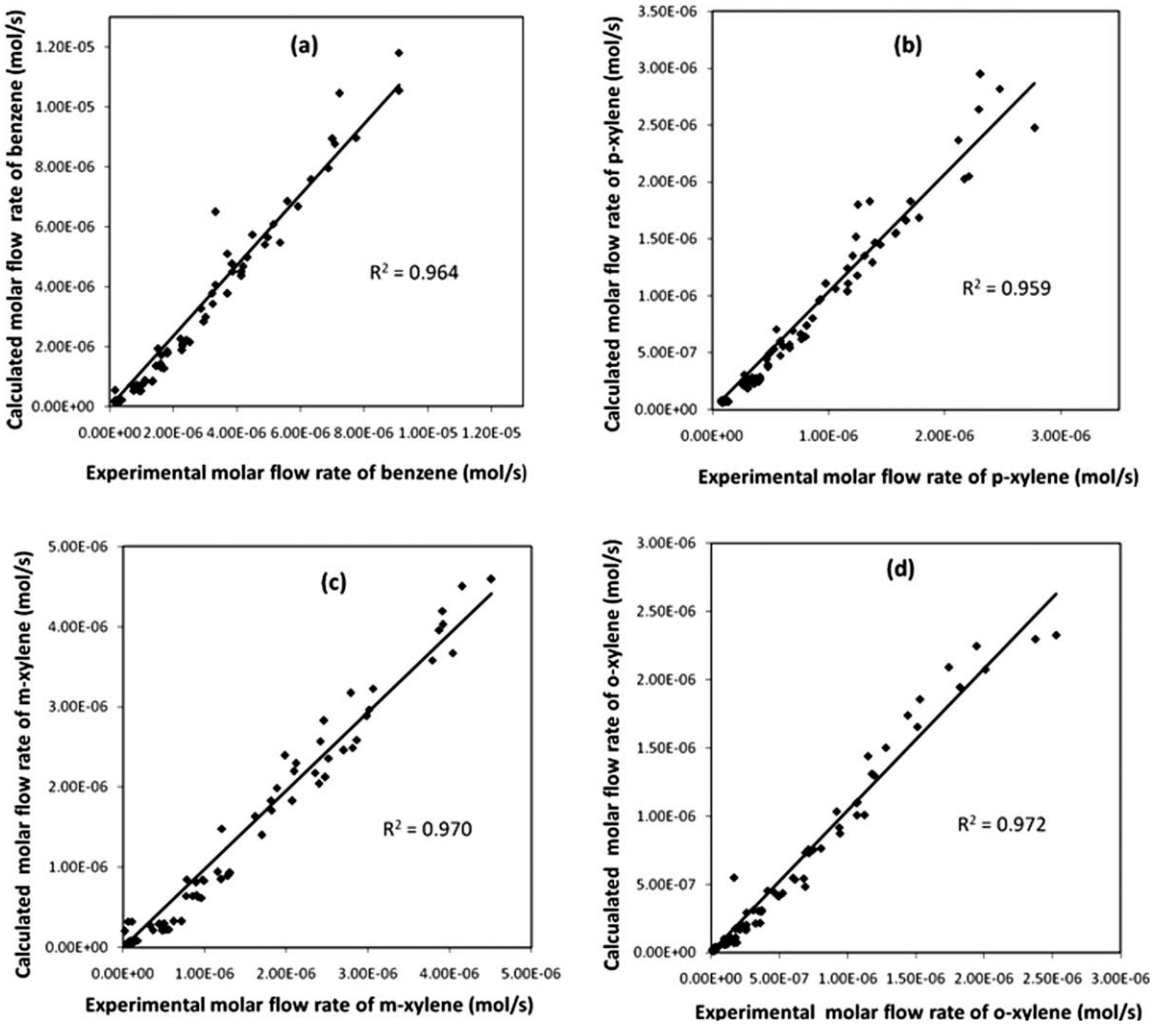


**Figure 9. Comparison of experimental and calculated molar flow rates of products (Temperature: 573–723 K): (a) Benzene, (b) *p*-xylene, (c) *m*-xylene, and (d) *o*-xylene.**

diffusivity estimated at 773 K from the above data was used in the Weisz-Prater criterion. This resulted in the left hand side being equal to 0.0004, which satisfies the Weisz-Prater criterion for second-order reactions. This shows that the concentration gradient in the zeolite crystal was insignificant and the entire volume of the zeolite crystal was effective in the toluene disproportion reaction. Beltrame et al.[20] and Uguina et al.[31] also found negligible intracrystalline diffusion resistance in the ZSM5 channels for the toluene disproportionation reaction. Intracrystalline diffusion in zeolite crystals was also found to be insignificant by Herring et al.[59] for the reaction of methanol or dimethylether to hydrocarbons over ZSM5 catalysts.

The ZSM5 crystals agglomerate to form powder particles with intercrystalline pores in the range of 3.6–5.7 nm, as determined from the pore-size distribution data of the milled ZSM5 powder. The relative importance of diffusional influences in the intercrystalline pores and zeolite channels (intracrystalline pores) was evaluated by determining $D_e/R_p^2$ for the powder (average size: 2.5 $\mu$m) and the zeolite crystals (average size: 37.34 nm).[55] The effective diffusivity in the intercrystalline pores was calculated using the random pore model by considering both bulk and Knudsen diffusion.[60] The intercrystalline porosity was assumed to be 0.5. Calculations showed that for these conditions, Knudsen diffusion was controlling and $D_e$ in the intercrystalline pores at 773 K was in the range of $1.63 \pm 0.37 \times 10^{-7}$ m$^2$/s. The $D_e$ in the intracrystalline pores of the ZSM5 crystal was $9.91 \times 10^{-12}$ m$^2$/s, as estimated earlier. Thus, $D_e/R_p^2$ for the zeolite crystals and the powder were $7.11 \times 10^3$ and $1.04 \times 10^5$, respectively. This shows that the diffusion rate in the intracrystalline pores was slower than that in the intercrystalline pores. As discussed earlier, the Weisz-Prater criterion was satisfied for the crystals which had a slower diffusion rate; therefore, it can be reasoned that the diffusion resistance in the intercrystalline pores in the powder particles was also negligible.

To estimate the diffusional resistance in the washcoat it is essential to know the effective diffusivity of the reactant and product gases in the washcoat. Earlier studies have revealed that knowledge of the washcoat characteristics is essential to correctly represent the rate of diffusion in the washcoat.[30] Diffusion could be dominated by bulk or Knudsen diffusion or a combination of the two depending on the size of the pores in the washcoat matrix. The two commonly used

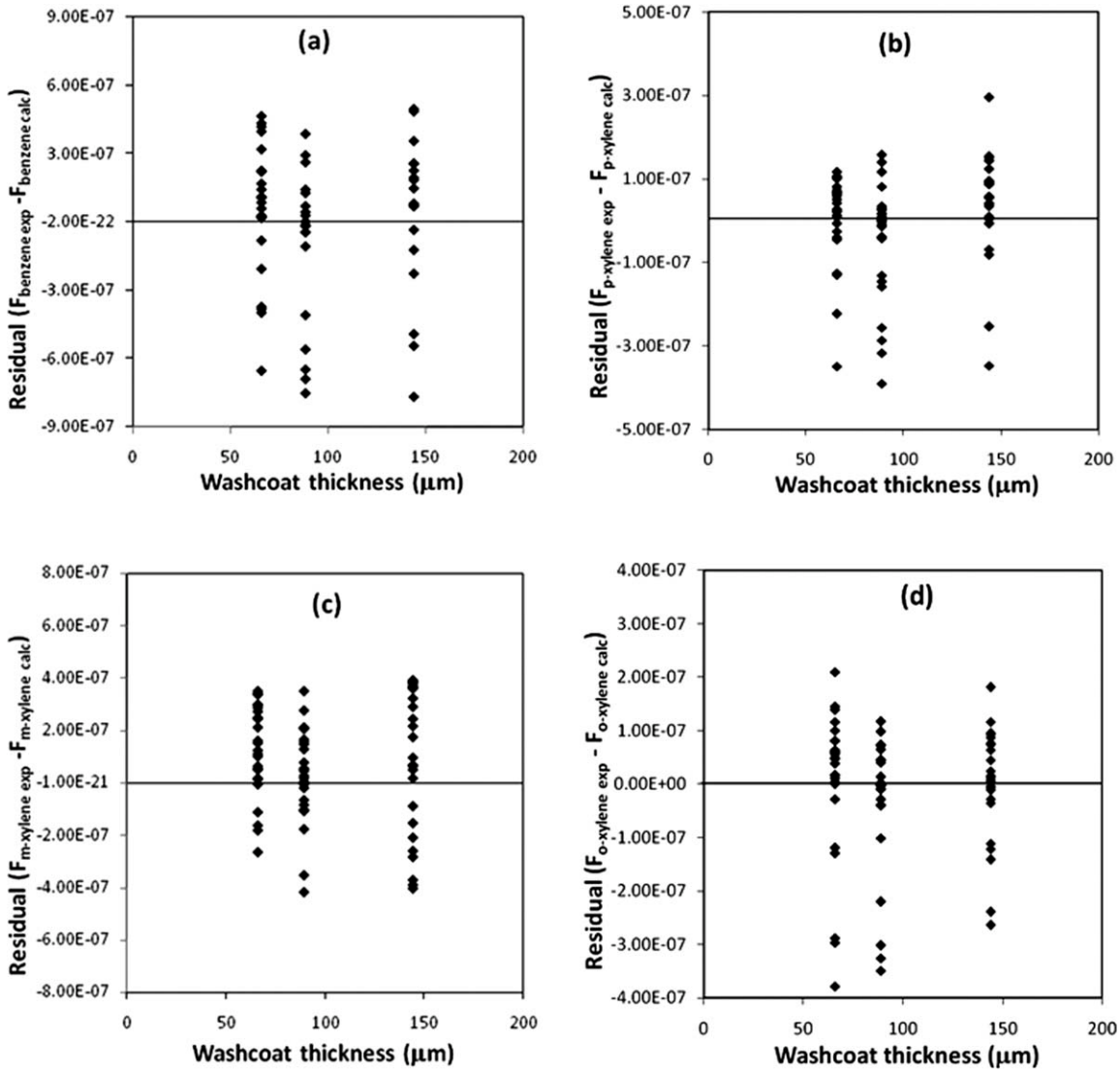


**Figure 10. Variation of residuals with zeolite washcoat thickness: (a) Benzene, (b) *p*-xylene, (c) *m*-xylene, and (d) *o*-xylene.**

models to estimate the effective diffusivity are the parallal pore model and the random pore model. Although there are no studies on experimental measurement of effective diffusivity in a zeolite washcoat, there are some reports of experimental studies carried out on $\gamma$-alumina and three-way catalyst washcoats. Hayes et al.[61] measured the effective diffusivity of methane in nitrogen through alumina washcoat and cordierite, and compared it with the values obtained from parallel-pore and random pore model. They showed that values calculated from the random pore model were 3–7 times larger than the measured values. Values calculated from the parallel-pore model were in good agreement with the experimental results when the tortuosity values of 8.1–8.5 were used. These values are larger than what is usually used for porous systems. Hence, estimation of effective diffusivity by either of the models has its own limitations. In this model, the effective diffusivities of the components in the zeolite washcoat were taken as adjustable parameters for estimating the outlet product composition for disproportionation of toluene using monoliths of varying washcoat thickness.

Comparison of the calculated and experimental conversions of toluene as a function of $W/F_{Ao}$ at 723 K is presented in Figure 8 for washcoat loadings of 28, 41, and 60 wt %. The experimental and calculated molar flow rates of benzene, *p*-xylene, *m*-xylene, and *o*-xylene in the temperature range of 573 and 723 K are compared in Figure 9. The reasonably good fit shows that the model could satisfactorily predict the experimentally measured toluene conversion and product molar flow rates for all the runs. To further check the adequacy of the model, the residuals were plotted against zeolite washcoat thickness and are shown in Figure 10 for all temperatures. The residuals were found to be scattered both above and below the reference line for all products and washcoat thicknesses. The residuals did not exhibit any systematic variation confirming that the model represented the data adequately.

The statistical significance of the model and its adequacy were tested by means of the *F*-tests for regression and lack of fit. For regression, the *F*-ratio was calculated as the ratio

**Table 4. Estimated Effective Diffusivities From Model**

| Temperature (K) | Diffusivity of the Different Components ($m^2/s$) | | | | | | |
|---|---|---|---|---|---|---|---|
| | Toluene | Benzene | *p*-Xylene | *m*-Xylene | *o*-Xylene | Gaseous Hydrocarbons | $\varepsilon$ |
| 573 | $1.57 \times 10^{-7}$ | $1.25 \times 10^{-7}$ | $1.09 \times 10^{-8}$ | $1.19 \times 10^{-8}$ | $1.96 \times 10^{-8}$ | $3.57 \times 10^{-7}$ | 0.284 |
| 623 | $4.77 \times 10^{-7}$ | $2.27 \times 10^{-7}$ | $2.50 \times 10^{-8}$ | $3.58 \times 10^{-8}$ | $4.78 \times 10^{-8}$ | $6.16 \times 10^{-7}$ | 0.522 |
| 673 | $6.93 \times 10^{-7}$ | $4.31 \times 10^{-7}$ | $4.02 \times 10^{-8}$ | $6.59 \times 10^{-8}$ | $7.19 \times 10^{-8}$ | $8.62 \times 10^{-7}$ | 0.188 |
| 723 | $8.01 \times 10^{-7}$ | $9.15 \times 10^{-7}$ | $9.06 \times 10^{-8}$ | $9.71 \times 10^{-8}$ | $1.03 \times 10^{-7}$ | $1.04 \times 10^{-6}$ | 0.233 |

of the regression sum of squares and the residual sum of squares, whereas for lack of fit, the *F*-ratio was the ratio of sum of squares due to lack of fit and the sum of squares due to pure error.[62] The calculated values showed that at all temperatures the regression was significant, as the *F*-ratio calculated for regression was greater than the *F*-statistic value and the lack of fit was not significant, as the *F*-ratio of lack of fit to pure error was less than the *F*-statistic value at a 95% confidence level.

The estimated values of the effective diffusivities of the different species between 573 and 723 K along with the average relative errors ($\varepsilon$) are given in Table 4. The pore-size distribution in the zeolite washcoat in the monoliths revealed pore sizes in the range of 18.5–40 nm. The effective diffusivity values estimated in this study indicate that Knudsen diffusion is controlling in the washcoat. No published information is available on the experimental determination of effective diffusivities in zeolite washcoats. However, the values of the effective diffusivities determined in the studies on $\gamma$-alumina and three-way catalyst washcoats revealed that Knudsen diffusion was dominant in the washcoat pores.[30,62,63] The estimation of the different diffusion resistances in the washcoat indicate that the slowest mass transfer step in this washcoated monolith reactor is the diffusion through the pores in the washcoat, rather than intercrystalline diffusion, intracrystalline diffusion or external mass transfer.

Further, the data at 773 K was used to check the predictive capacities of the model. Using the effective diffusivities estimated as above at four temperatures (573, 623, 673, and 723 K) and assuming an Arrhenius dependency, the effective diffusivities of the different components at 773 K were determined. These values were then used in the model to calculate the outlet molar percentages of the products for 41 wt % ZSM5-coated monolith at 773 K and the results are shown in Figure 11.

The variation of effectiveness factor of the first reaction (toluene disproportionation step, Eq. 1) with temperature for the three washcoat thickness calculated at the entrance of the reactor is shown in Figure 12. Because, the temperature dependence of the reaction rate is stronger than that of the diffusivity, the effectiveness factor decreases with increasing temperature. The effectiveness factor decreased with an increase in washcoat thickness due to higher diffusional resistance in the washcoat.

## Conclusions

ZSM5-coated monoliths with loading ranging from 10 to 60 wt % are active for the toluene disproportionation reaction. Toluene conversion is enhanced by increasing temperature and $W/F_{Ao}$, similar to a ZSM5 powder catalyst. An increase in washcoat thickness, however, decreases conversion as thicker washcoats result in an enhancement of diffusional limitations. Use of monoliths lead to products (benzene, xylene isomers, and gaseous hydrocarbons) similar to packed bed reactors. The monolith catalysts are selective for *p*-xylene and the para selectivity is higher than the equilibrium value. The *p*-xylene selectivity depends on temperature and washcoat thickness. The high *p*-xylene selectivity, especially, for monoliths with thin washcoats is most likely due to the quick and efficient diffusion of the initially formed *p*-xylene from the

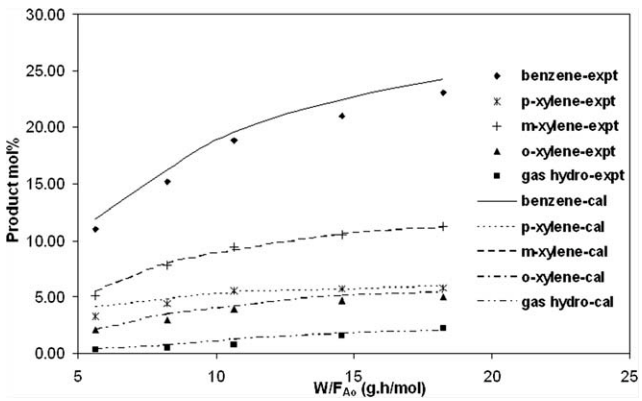


**Figure 11. Comparison between experimental and calculated mol % products for 41 wt % ZSM5-coated monolith (Temperature: 773 K).**

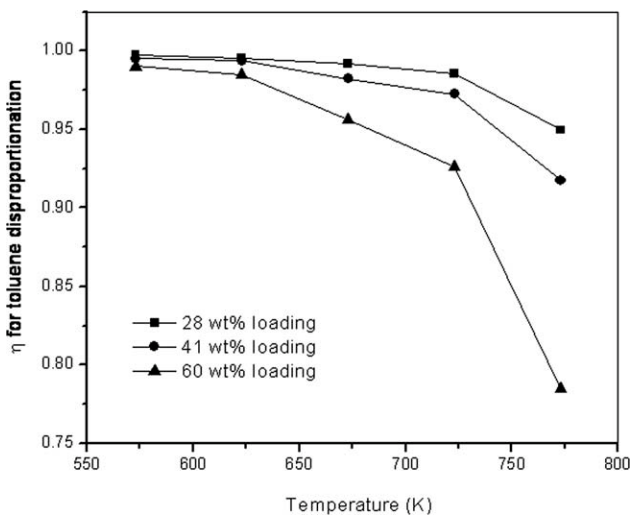


**Figure 12. Variation of effectiveness factor for toluene disproportionation step (Eq. 1) with temperature.**

zeolite pores into the bulk gas phase preventing further isomerization of the primary product.

A four step reaction scheme can satisfactorily represent the product distribution for toluene disproportionation in monoliths. Kinetic constants determined for these reactions for the 10 wt % ZSM5-coated monolith are found to be in agreement with previously reported literature values. A one-dimensional reactor model, coupled with a module to determine the concentration profile in the catalyst washcoat, can satisfactorily predict the performance of the monolith reactor for this reaction. The estimated values of the effective diffusivities in the catalyst washcoat show that Knudsen diffusion is controlling in the pores of the washcoat. The intracrystalline diffusion resistance in the ZSM5 crystals and the intercrystalline diffusion in the powder are negligible for this reaction and the effective diffusivity is mainly limited by diffusion through the washcoat pores. The results of this study should be helpful in determining the optimum conditions for enhancing the yield of *p*-xylene from disproportionation of toluene.

## Notation

$a_m$ = geometrical surface area of monolith ($m^{-1}$)
$A$ = flow area in the monolith channels ($m^2$)
$A_{ik}$ = discretization coefficient matrix for orthogonal collocation
$B_{ik}$ = discretization coefficient matrix for orthogonal collocation
$C_i$ = concentration of component $i$ (mol $m^{-3}$)
$C_{i,b}$ = concentration of component $i$ in bulk gas phase (mol $m^{-3}$)
$C_{i,k}$ = concentration of component $i$ at the $k$th collocation point (mol $m^{-3}$)
$C_s$ = reactant concentration at the external surface of the particle (mol $m^{-3}$)
$D_{con}$ = configurational diffusivity ($m^2$ $s^{-1}$)
$D_e$ = effective diffusivity ($m^2$ $s^{-1}$)
$D_{e,i}$ = effective diffusivity of component $i$ ($m^2$ $s^{-1}$)
$E$ = activation energy of configurational diffusivity (J $mol^{-1}$ $K^{-1}$)
$F_i$ = molar flow rate of component $i$ (mol $s^{-1}$)
$F_{io}$ = molar flow rate of component $i$ at the inlet (mol $s^{-1}$)
$F_{H_2}$ = molar flow rate of hydrogen (mol $s^{-1}$)
$F_o$ = total molar flow rate at the inlet (mol $s^{-1}$)
$H$ = partition coefficient (dimensionless)
$\Delta H$ = heat of adsorption (J $mol^{-1}$ $K^{-1}$)
$k_j$ = rate constant for the forward reaction (mol $kg^{-1}$ $s^{-1}$ $Pa^{-n}$)
$k_{-j}$ = rate constant for the backward reaction (mol $kg^{-1}$ $s^{-1}$ $Pa^{-n}$)
$K_j$ = thermodynamic equilibrium constants for the reaction (dimensionless)
$L$ = reactor length (m)
$L_c$ = average washcoat thickness ($\mu$m)
$n$ = the order of the reaction
$N$ = number of collocation points
$P$ = reaction pressure (Pa)
$p_i$ = partial pressures of species (Pa)
$R$ = universal gas constant (J $mol^{-1}$ $K^{-1}$)
$R_p$ = radius of the catalyst particle (m)
$r_j$ = rate of reaction $j$ (mol $kg^{-1}$ $s^{-1}$)
$r_{j,k}$ = rate of reaction $j$ at the $k$th collocation point (mol $kg^{-1}$ $s^{-1}$)
$R_i$ = rate of formation of component $i$ (mol $kg^{-1}$ $s^{-1}$)
$R_{i,k}$ = rate of formation of component $i$ at the $k$th collocation point (mol $kg^{-1}$ $s^{-1}$)
$R_{obs}$ = observed rate of reaction per unit particle volume (mol $m^{-3}$ $s^{-1}$)
$r_p$ = radius of the particle (m)
$T$ = reaction temperature (K)
$W$ = weight of ZSM5 loaded on monolith (kg)
$x$ = normalized coordinate in the washcoat (dimensionless)
$x_c$ = catalyst volume fraction (dimensionless)
$y_i$ = mole fraction species $i$ (dimensionless)
$z$ = axial coordinate of monolith reactor (m)

### *Greek letters*

$\alpha_{ij}$ = stoichiometric coefficient of $i$th component of $j$th reaction
$\varepsilon$ = average relative error (dimensionless)
$\varepsilon_m$ = void fraction (dimensionless)
$\eta_i$ = effectiveness factor for component $i$ (dimensionless)
$\eta_j$ = effectiveness factor for reaction $j$ (dimensionless)
$\rho_B$ = washcoat density of the monolith (kg $m^{-3}$ of monolith)
$\rho_c$ = density of the ZSM5 washcoat (kg $m^{-3}$ of washcoat)
$\omega_{ik}$ = quadrature weightage (dimensionless)

## Literature Cited


1. Heck RM, Gulati S, Farrauto RJ. The application of monoliths for gas phase catalytic reactions. *Chem Eng J*. 2001;82:149–156.
2. Cybulski A, Moulijn JA, editors. *Structured Catalysts and Reactors*. New York: Marcel Dekker Inc., 1998.
3. Irandoust S, Andersson B. Monolithic catalysts for non-automobile applications. *Catal Rev Sci Eng*. 1988;30:341–392.
4. Davis ME. Zeolite-based catalysts for chemicals synthesis. *Microporous Mesoporous Mater*. 1998;21:173–182.
5. Nijhius TA, Beers AEW, Vergunst T, Hoek I, Kapteijn F, Moulijn JA. Preparation of monolithic catalysts. *Catal Rev Sci Eng*. 2001;43: 345–380.
6. Zamaro JM, Ulla MA, Miro EE. Zeolite washcoating onto cordierite honeycomb reactors for environmental applications. *Chem Eng J*. 2005;106:25–33.
7. Mitra B, Kunzru D. Washcoating of different zeolites in cordierite monoliths. *J Am Ceram Soc*. 2008;91:64–70.
8. Chen HY, Voskoboinikov T, Sachtler WMH. Reduction of $NO_x$ over Fe/ZSM-5 catalysts: mechanistic causes of activity differences between alkanes. *Catal Today*. 1999;54:483–494.
9. Tomasic V, Gomzi Z. Experimental and theoretical study of NO decomposition in a catalytic monolith reactor. *Chem Eng Process*. 2004;43:765–774.
10. Antia JE, Israni K, Govind R. *n*-Hexane cracking on binderless zeolite HZSM-5 coated monolithic reactors. *Appl Catal A*. 1997;159: 89–99.
11. Antia JE, Govind R. Conversion of methanol to gasoline-range hydrocarbons in a ZSM-5 coated monolithic reactor. *Ind Eng Chem Res*. 1995;34:140–147.
12. Parikh PA. Catalytic and kinetic study of toluene ethylation over ZSM-5 washcoated honeycomb monolith. *Ind Eng Chem Res*. 2008; 47:1793–1797.
13. Hilmen AM, Bergene EO, Lindvag A, Schanke D, Eri S, Holmen A. Fischer-Tropsch synthesis on monolithic catalysts of different materials. *Catal Today*. 2001;61:227–232.
14. Vergunst T, Kapteijn F, Moulijn JA. Optimization of geometric properties of a monolithic catalyst for the selective hydrogenation of phenylacetylene. *Ind Eng Chem Res*. 2001;40:2801–2809.
15. Garcia-Bordeje E, Calvillo L, Lazaro MJ, Moliner R. Study of configuration and coating thickness of vanadium on carbon-coated monoliths in the SCR of NO at low temperatures. *Ind Eng Chem Res*. 2004;43:4073–4079.
16. Kapteijn F, de Deugd RM, Moulijn JA. Fischer-Tropsch synthesis using monolithic catalysts. *Catal Today*. 2005;105:350–356.
17. Chen NY, Garwood WE, Dwyer FG. *Shape Selective Catalysis in Industrial Applications*. New York: Marcel Dekker, 1989.
18. Bhavikatti SS, Patwardhan SR. Toluene disproportionation over nickel-loaded aluminum deficient mordenite. 2. Kinetics. *Ind Eng Chem Prod Res Dev*. 1981;20:106–109.
19. Aneke LE, Gerritsen LA, Eilers J, Trion R. The disproportionation of toluene over a HY/b-$AlF_3$/Cu catalyst. 2. Kinetics. *J Catal*. 1979; 59:37–44.
20. Beltrame P, Beltrame PL, Carniti P, Forni L, Zuretti G. Toluene disproportionation catalysed by various zeolites. *Zeolites*. 1985;5:400–405.
21. Young LB, Butter SA, Kaeding WW. Shape-selective reactions with zeolite catalysts. III. Selectivity in xylene isomerization, toluene-methanol alkylation, and toluene disproportionation over ZSM-5 zeolite catalysts. *J Catal*. 1982;76:418–432.
22. Meshram NR, Hedge SG, Kulkarni SB, Ratnasamy P. Disproportionation of toluene over HZSM-5 zeolites. *Appl Catal*. 1983;8:359–367.

23. Olson DH, Haag WO. Structure-selectivity relationship in xylene isomerization and selective toluene disproportionation. *ACS Symp Ser* 1984;14:275–307.
24. Kaeding WW, Chu C, Young LB, Weinstein B, Butter SA. Selective alkylation of toluene with methanol to produce *p*-xylene. *J Catal*. 1981;67:159–174.
25. Tsai TC, Liu SB, Wang I. Disproportionation and transalkylation of alkylbenzenes over zeolite catalysts. *Appl Catal A*. 1999;181: 355–398.
26. Kaeding WW, Chu C, Young LB, Butter SA. Shape-selective reactions with zeolite catalysts. II. Selective disproportionation of toluene to produce benzene and *p*-xylene. *J Catal*. 1981;69:392–398.
27. Sugi Y, Kubota Y, Komura K, Sugiyama N, Hayshi M, Kim J-H, Seo G. Shape selective alkylation and related reactions of mononuclear aromatic hydrocarbons over H-ZSM-5 zeolites modified with lanthanum and cerium oxides. *Appl Catal A*. 2006;299:157–166.
28. Chen J, Yang H, Wang N, Ring Z, Dabros T. Mathematical modeling of monolith catalysts and reactors for gas phase reactions. *Appl Catal A*. 2008;345:1–11.
29. Hayes RE, Kolaczkowski ST. Mass and heat transfer effects in catalytic monolithic reactors. *Chem Eng Sci*. 1994;49:3587–3599.
30. Zhang F, Hayes RE, Kolaczkowski ST. A new technique to measure the effective diffusivity in a catalytic monolith washcoat. *Chem Eng Res Des*. 2004;84:485–489.
31. Uguina MA, Sotelo JL, Serrano DP. Kinetics of toluene disproportionation over unmodified and modified ZSM-5 zeolites. *Ind Eng Chem Res*. 1993;32:49–55.
32. Bhaskar GV, Do DD. Toluene disproportionation reaction over ZSM-5 zeolites: kinetics and mechanism. *Ind Eng Chem Res*. 1990; 29:355–361.
33. Nayak US, Riekert L. Catalytic activity and product distribution in the disproportionation of toluene on different preparations of pentasil zeolite catalysts. *Appl Catal*. 1986;23:403–411.
34. Al-Khattaf S. Xylene reactions and diffusions in ZSM-5 zeolite based catalyst. *Ind Eng Chem Res*. 2007;46:59–69.
35. Kunnieda T, Kim J-H, Niwa M. Source of selectivity of *p*-xylene formation in the toluene disproportionation over HZSM-5 zeolites. *J Catal*. 1999;188:431–433.
36. Cortes A, Corma A. Kinetics of the gas-phase catalytic isomerization of xylenes. *Ind Eng Chem Process Des Dev*. 1980;19:263–267.
37. Bauer F, Chen W-H, Ernst H, Huang S-J, Freyer A, Liu S-B. Selectivity improvement in xylene isomerization. *Microporous Mesoporous Mater*. 2004;72:81–89.
38. Rao YVC. *Chemical Engineering Thermodynamics*. New Delhi: Universities Press (India) Pvt. Ltd., 1997.
39. Das J, Bhat YS, Halgeri AB. Selective toluene disproportionation over pore size controlled MFI zeolite. *Ind Eng Chem Res.* 1994;33:246–250.
40. Li Y, Chang X, Zeng Z. Kinetic study of the isomerization of xylene on ZSM-5 zeolite. 1. Kinetic model and reaction mechanism. *Ind Eng Chem Res*. 1992;31:187–192.
41. Choi H, Ham S-W, Nam I-S, Kim YG. Honeycomb reactor washcoated with mordenite type zeolite catalysts for the reduction of $NO_x$ by $NH_3$. *Ind Eng Chem Res*. 1996;35:106–112.
42. Beckman JW, Hegedus LL. Design of monolith catalysts for power plant $NO_x$ emission control. *Ind Eng Chem Res*. 1991;30:969–978.
43. Jarvi GA, Mayo KB, Bartholomew CH. Monolith-supported nickel catalysts. 1. Methanation activity relative to pellet catalysts. *Chem Eng Commun*. 1980;4:325–341.
44. Heck RH, Wei J, Katzer JR. Mathematical modeling of monolithic catalysts. *AIChE J*. 1976;22:477–484.
45. Santos H, Costa M. The relative importance of external and internal transport phenomena in three way catalysts. *Int J Heat Mass Transfer*. 2008;51:1409–1422.
46. Leung D, Hayes RE, Kolaczkowski ST. Diffusion limitation in the washcoat of a catalytic monolith reactor. *Can J Chem Eng*. 1996;74:94–103.
47. Hayes RE, Liu B, Moxom R, Votsmeier M. The effect of washcoat geometry on mass transfer in monolith reactors. *Chem Eng Sci*. 2004;59:3169–3181.
48. Santos H, Costa M. Modeling transport phenomena and chemical reactions in automotive three-way catalytic convertors. *Chem Eng J*. 2009;148:173–183.
49. Berger RJ, Kapteijn F. Coated-wall reactor modeling-criteria for neglecting radial concentration gradients. 1. Empty reactor tubes. *Ind Eng Chem Res*. 2007;46:3863–3870.
50. Roy S, Heibel AK, Liu W, Boger T. Design of monolithic catalysts for multiphase reaction. *Chem Eng Sci*. 2004;59:957–966.
51. Gupta SK. *Numerical Methods for Engineers*. New Delhi: New Age international (P) Ltd., 1995.
52. Mears DE. Tests for transport limitations in experimental catalytic reactors. *Ind Eng Chem Process Des Dev*. 1971;10:541–547.
53. Ruthven DM. *Principles of Adsorption and Absorption Processes*. USA: Wiley, 1984.
54. Xiao J, Wei J. Diffusion mechanism of hydrocarbons in zeolites—II. Analysis of experimental observations. *Chem Eng Sci*. 1992;47: 1143–1159.
55. Masuda T. Diffusion mechanisms of zeolite catalysts. *Catal Surv Asia*. 2003;7:133–144.
56. Masuda T, Hashomoto K. Measurements of adsorption on outer surface of zeolite and their influence on evaluation of intracrystalline diffusivity. *Stud Surf Sci Catal*. 1993;83:225–232.
57. Masuda T, Fujikata Y, Nishida T, Hashimoto K. The influence of acid sites on intracrystalline diffusivities within MFI-type zeolites. *Microporous Mesoporous Mater*. 1998;23:157–167.
58. Avila AV, Bidabehere CM, Sedran U. Diffusion and adsorption selectivities of hydrocarbons over FCC catalysts. *Chem Eng J*. 2007; 132:67–75.
59. Herring J, Kotter M, Reikert L. Diffusion and catalytic reaction in zeolite ZSM-5. *Chem Eng Sci*. 1982;37:581–584.
60. Smith JM. *Chemical Engineering Kinetics*. Japan: McGraw Hill International Book Company, 1981.
61. Hayes RE, Kolaczkowski ST, Li PKC, Awdry S. Evaluating the effective diffusivity of methane in the washcoat of a honeycomb monolith. *Appl Catal B*. 2000;25:93–104.
62. Mongtomery DC. *Design and Analysis of Experiments*. USA: Wiley, 2001.
63. Stary T, Solcova O, Schneider P, Marek M. Effective diffusivities and pore-transport characteristics of washcoated ceramic monolith for automotive catalytic converter. *Chem Eng Sci*. 2006;61:5934–5943.

*Manuscript received July 2, 2010, and revision received Nov. 15, 2010.*